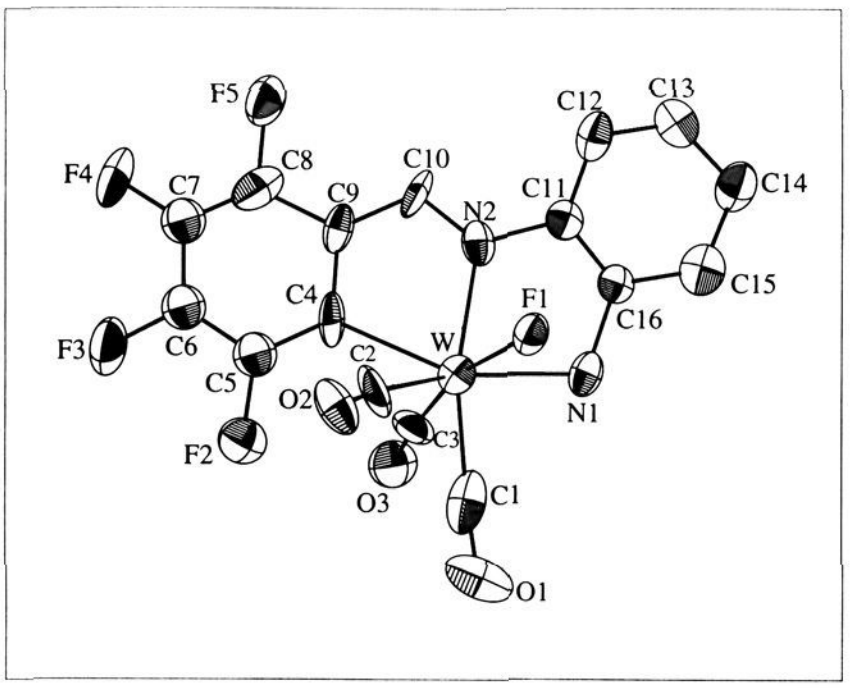

Figure 1. ORTEP representation of **3** with THF solvate omitted. Selected bond distances (Å) are as follows: W-N1, 2.250 (5); W-N2 2.182 (6); W-C1, 2.03 (1); W-C2, 1.947 (8); W-C3, 1.859 (7); N2-C10, 1.265 (8). Selected bond angles (deg) are as follows: F1-W-C4, 125.5 (2); N1-W-N2, 75.2 (2); N2-W-C4, 73.1; N2-W-C1, 164.6 (2); N1-W-C2; 155.1 (3); F1-W-C3, 165.1 (3).

in several higher oxidation state compounds,[13] the width of the resonance hinders the detection of ^{183}W satellites. The strongly deshielded resonance at −111.44 ppm is assigned[14] to F^2 (see Scheme I) and exhibits an additional coupling to the imine proton of the ligand ($^5J_{HF}$ = 1.9 Hz). Selective ^{19}F decoupling of this resonance causes the imine to collapse to a singlet clearly revealing ^{183}W satellites ($^3J_{WH}$ = 8.8 Hz). This coupling is indicative of metallocycle formation in related ligand systems.[8] Aside from the aromatic backbone of the ligand, diastereotopic NH protons are observed at 6.52 and 6.30 ppm. Addition of D_2O results in rapid proton exchange of the amine hydrogens as evidenced by ^1H NMR spectra.

The solid-state structure of **3** is illustrated in Figure 1.[15] The geometry of the seven-coordinate complex can be approximated as a capped octahedron with C4 as the capping atom.[16] The W-C4(2.232 (6) Å)[8] and W-F1(2.032 (4) Å)[17] bond lengths appear to be normal. The five-membered metallacycle is planar with the largest deviation from the least-squares plane being 0.09 Å. Indeed, the entire ligand (15 atoms) is planar within ±0.25 Å; the tungsten atom is located 0.72 Å from this plane.

The mechanism of this reaction is under investigation. Intermediate **2** can be isolated as a dark purple solid in 82% yield by conducting the reaction in CH_2Cl_2 followed by immediate precipitation with hexanes.[18] Transformation of **2** to **3** is rapid in THF at room temperature. However, dissolution of **2** in CH_3CN affords **1** and $W(CO)_3(NCCH_3)_3$. Low-temperature ^{19}F NMR studies of **2** in acetone-d_6 did not provide any evidence for fluorocarbon binding to tungsten,[19] but studies in less coordinating solvents proved difficult because of the low solubility and high reactivity of **2**.

Several factors probably account for the remarkably facile C-F oxidative addition process described above. The nitrogen donor atoms of **1** afford the very basic metal center (as judged by low ν_{CO} values in the IR spectrum) required for oxidative addition in the intermediate **2**. The chelating nature of the ligand reduces the entropic barrier to reaction and the planar, conjugated metallacycle is quite stable.[8] In addition, the overall thermodynamic favorability of this transformation suggests that the tungsten(II)-fluoride bond is reasonably strong despite the low formal oxidation state of the metal.[20]

These results suggest that metal-catalyzed transformations of heavily fluorinated organic molecules may be possible despite the great strength of the carbon-fluorine bond. We are continuing to explore other carbon-heteroatom bond activation reactions in this and related systems.

Acknowledgment. T.G.R. is the recipient of a Distinguished New Faculty Grant from the Camille & Henry Dreyfus Foundation Inc. We are grateful for support from the donors of the Petroleum Research Fund administered by the American Chemical Society. High field NMR spectrometers employed in this work were obtained through departmental grants from the National Science Foundation. We thank Dr. Alan E. Sopchik for recording 400 MHz $^1H\{^{19}F\}$ NMR spectra.

Supplementary Material Available: Full crystallographic data for **3**·THF including tables of bond distances and angles and final positional and thermal parameters (14 pages); listing of calculated and observed structure factors (19 pages). Ordering information is given on any current masthead page.

(12) (a) Nesmeyanov, A. N.; Nogina, O. V.; Fedin, E. I.; Dubovitskii, V. A.; Kvasov, B. A.; Petrovskii, P. V. *Dokl. Chem. Proc. Acad. Sci. USSR, Chemistry Section* **1972**, *205*, 632-636. *Dokl. Akad. Nark SSSR* **1972**, *205*, 857-860. (b) Buffin, B. P.; Richmond, T. G., unpublished results, **1987**.

(13) (a) Wray, V. *Ann. Rep. NMR Spec.* **1983**, *14*, 365. (b) Postel, U.; Riess, J. G.; Calves, J. Y.; Guerchais, J. *Inorg. Chim. Acta* **1979**, *32*, 175-180.

(14) Bruce, M. I. *J. Chem. Soc. A* **1968**, 1454-1464.

(15) Crystal data for **3**·THF: $WF_5O_4N_2C_{20}H_{15}$, yellow, monoclinic, $P2_1/a$, a = 9.228 (9) Å, b = 16.814 (13) Å, c = 13.800 (8) Å, β = 105.05 (6)°, V = 2067.9 Å^3, Z = 4, Mo Kα of 3030 reflections collected at ambient temperature (Syntex P$\bar{1}$, 3° < 2θ < 45°) were unique of which 1971 had $F° > 2\sigma F°$ and were used in the solution (Patterson) and refinement. Final refinement included all non-hydrogen atoms as anisotropic contributions except for C5 and C7 which were refined as isotropic contributions (279 variables). For parameters, R = 0.084 and R_w = 0.088, GOF = 2.7, and highest peak in the final map of 1.3 e Å^{-3} approximately 1.3 Å from W.

(16) Drew, M. G. B. *Prog. Inorg. Chem.* **1977**, *23*, 67-210. Hoffmann, R.; Beier, B. F.; Muetterties, E. L.; Rossi, A. R. *Inorg. Chem.* **1977**, *16*, 511-522.

(17) Hidai, M.; Mizobe, Y.; Sato, M.; Kodama, T.; Uchida, Y. *J. Am. Chem. Soc.* **1978**, *100*, 5740-5748.

(18) NMR data for **2** at 0 °C: ^{19}F (acetone-d_6, CCl_3F reference) −138.90 (d, 2 F), −154.65 (t, 1 F), −162.25 (m, 2 F); ^1H (acetone-d_6) 9.20 (s, 1 H), 7.71 (d, 1 H), 7.46 (m, 3 H), 6.21 (d, 1 H), 5.63 (d, 1 H).

(19) (a) Kulawiec, R. J.; Holt, E. M.; Lavin, M.; Crabtree, R. H. *Inorg. Chem.* **1987**, *26*, 2559-2561. (b) Uson, R.; Fornies, J.; Tomas, M.; Cotton, F. A.; Falvello, L. R. *J. Am. Chem. Soc.* **1984**, *106*, 2482-2483. (c) Catala, R. M.; Cruz-Garritz, D.; Hills, A.; Hughes, D. L.; Richards, R. L.; Sosa, P.; Torrens, H. *J. Chem. Soc., Chem. Commun.* **1987**, 261-262.

(20) For a recent discussion of the stability of low valent metal fluorides, see: Branan, D. M.; Hoffman, N. W.; McElroy, E. A.; Miller, N. C.; Ramage, D. L.; Schott, A. F.; Young, S. H. *Inorg. Chem.* **1987**, *26*, 2915-2917.

Free Energy Perturbation Method for Chemical Reactions in the Condensed Phase: A Dynamical Approach Based on a Combined Quantum and Molecular Mechanics Potential

Paul A. Bash,* Martin J. Field,* and Martin Karplus*

Department of Chemistry, Harvard University
Cambridge, Massachusetts 02138

Received July 20, 1987

Dynamical simulations are necessary for a full understanding of the effect of the environment on the behavior of chemical reactions in solution[1,2] and the active sites of enzymes.[3,4] We have developed a molecular dynamics simulation methodology based on combined quantum and molecular mechanics potentials for addressing the general problem of chemical reactions in the condensed phase. In what follows we give a brief outline of the method and apply it to the S_N2 reaction $Cl^- + CH_3Cl$ in the gas phase and in solution.

(1) Chandrasekhar, J.; Smith, S. F.; Jorgensen, W. L. *J. Am. Chem. Soc.* **1985**, *107*, 154.

(2) Bergsma, J. P; Gartner, B. J.; Wilson, K. R.; Hynes, J. T. *J. Chem. Phys.* **1987**, *86*, 1356.

(3) Northrup, S. H.; Pear, M. R.; Lee, C.-Y.; McCammon, J. A.; Karplus, M. *Proc. Natl. Acad. Sci. U.S.A.* **1982**, *79*, 4035.

(4) Brünger, A.; Brooks, C. B.; Karplus, M. *Proc. Natl. Acad. Sci. U.S.A.* **1985**, *82*, 8458.

0002-7863/87/1509-8092$01.50/0

Table I. Thermodynamics of Reaction $Cl^-\cdots CH_3Cl$[a]

Energies and Free Energies (kcal/mol)

method	$\Delta G(A \rightarrow B)$	$\Delta G_{solv}(A \rightarrow B)$	$\Delta G_{gas}(A \rightarrow B)$	$E_{quantum}(A)$	$E_{quantum}(B)$
AM1 (VDW params)[b]	27.7	25.65	2.05	−179.2 ± 8.1	−131.6 ± 5.9
AM1 (no VDW params)	27.0	24.95	2.05	−177.5 ± 6.2	−122.2 ± 5.2
MNDO (no VDW params)	30.6	25.25	5.35	−199.4 ± 7.7	−138.9 ± 5.5
ab initio/mol. mech[c]	26.6				
experimental[d]	~26				

Gas-Phase Energy Differences (kcal/mol)

method	(complexation energy)	(intrinsic barrier)
AM1	−8.6	9.1
MNDO	−7.3	10.5
ab initio	−10.3[c]	13.9[c]
experimental	−8.5[e]	10–14[f]

[a] State A is the reactant state with the Cl^- atom at 6 Å from the CH_3Cl molecule, and state B is the optimized gas-phase transition-state geometry (C···Cl equal to 2.1545 Å). In the free energy simulations of ΔG, the solution free energy, and ΔG_{gas}, the gas phase free energy, the carbon atoms in the two states were coincident; the Cl^- ion and C atom were kept fixed in state A, and the two Cl atoms and the C atom were kept fixed in state B. The transformation was done in a series of simulations with $\Delta\lambda = 0.025$; each simulation consisted of 500 steps of equilibration followed by 500 steps of data collection; the simulation time step was 0.001 ps. $\Delta G_{solv}(A \rightarrow B)$ is the free energy change due to solvation and is calculated from $\Delta G(A \rightarrow B) - \Delta G_{gas}(A \rightarrow B)$. $E_{quantum}$ is the internal qm energy of the solute (state A or B) plus the (qm,mm) energy of interaction with solvent averaged over 500 steps. The complexation energy is the energy difference between the ion–dipole complex and the reactants; the intrinsic barrier is the energy difference between the transition state and the ion–dipole complex.[c] [b] Van der Waals parameters for CH_3 were $r^* = 1.8/\epsilon = -0.06$ and $r^* = 1.54/\epsilon = -0.01$ for carbon and hydrogen, respectively.[7d] Cl parameters, $r^* = 1.5/\epsilon = -0.4$, were chosen to fit the experimental interaction energy of $Cl^-(H_2O)_1$.[27] [c] See ref 1. [d] See ref 23. [e] See ref 24. [f] See ref 25.

Our approach couples a semiempirical quantum mechanical treatment[5,6] with molecular mechanics so that a system can be partitioned into quantum mechanical (qm) and molecular mechanical (mm) regions. The efficiency of the semiempirical method[8] enables one to calculate the combined quantum mechanical/molecular mechanical potential and forces at each step for use in classical dynamics simulations.[9] About 20 non-hydrogen (qm) atoms surrounded by several hundred (mm) atoms can be studied with available computational resources. For the (qm),(mm) interactions, the (mm) atoms are represented by a molecular mechanic partial (core) charge and no molecular orbitals. Electrostatic (qm),(mm) interactions are calculated by core(qm)/core(mm) and electron(qm)/core(mm) integrals which are added to the Hartree–Fock Hamiltonian that is then evaluated in the standard way; configuration interaction can be included if necessary. The van der Waals (VDW) interactions between (qm) and (mm) atoms can be treated by molecular mechanics, though the quantum mechanical core repulsion terms appear to be sufficient in some cases. Within the Born–Oppenheimer approximation, the total potential energy, $E_{(qm,mm)}$, and forces, $\mathbf{F}_{(qm,mm)}$, are obtained by adding the (mm) terms to the results of the quantum mechanical calculation for use in energy minimization, molecular dynamics, or Monte Carlo simulations.

Implementation of the method in the context of thermodynamic perturbation theory[10] requires a different Hamiltonian partitioning[11] from that used in most other formulations.[12-14] The system is divided into two states, A and B, described by Hamiltonian functions $\mathcal{H}_A$ and $\mathcal{H}_B$ that represent two "solute" groups, S_A and S_B, in the presence of a common "solvent" environment. In a free energy simulation, groups S_A and S_B exist simultaneously, and the transformation between states is carried out by using a mixed Hamiltonian $\mathcal{H}(\lambda) = \lambda\mathcal{H}_A + (1 - \lambda)\mathcal{H}_B$ where λ is a coupling parameter that takes on values from zero (pure B) to one (pure A). There is no interaction between S_A and S_B; all other energies and forces including S_A and S_B are scaled by λ and $(1 - \lambda)$, respectively.[11] With use of the mixed Hamiltonian, $\mathcal{H}(\lambda)$, the Helmholtz free energy change between two states, λ and $\lambda + \Delta\lambda$, is[10-16]

$$\Delta A_\lambda = -k_B T \ln \left\langle \exp\left(-\frac{\Delta E}{k_B T}\right)\right\rangle_\lambda$$

where k_B is the Boltzmann constant, T is the absolute temperature, $\Delta E = \Delta\lambda[E_{(qm,mm)}(A) - E_{(qm,mm)}(B)]$, and $\langle\ \rangle_\lambda$ represents a canonical average with $H(\lambda)$.

To test the method we apply it to the S_N2 reaction $Cl^- + CH_3Cl \rightarrow ClCH_3 + Cl^-$ in aqueous solution. An essential factor in the solvation is the nature of the charge transfer from the attacking Cl^- to CH_3Cl during the reaction. This can only be determined by a quantum mechanical calculation and may be affected by the presence of solvent. The free energy perturbation calculations were done with a version of the CHARMM program[17] modified to include $E_{(qm,mm)}$ and $\mathbf{F}_{(qm,mm)}$ terms,[18] with the quantum mechanical contributions evaluated by the MOPAC program.[19] Both the AM1[6] and MNDO[5] models were used for the gas-phase and solution calculations; the solution simulation was done in an equilibrated 11-Å sphere of 180 H_2O molecules with stochastic boundary conditions[4,20,21] at 300 K. The Cl^-, CH_3Cl system was treated quantum mechanically, and the TIP3P model[22] was employed for

(5) Dewar, M. J. S.; Thiel, W. *J. Am. Chem. Soc.* **1977**, *99*, 4899, 4907.
(6) Dewar, M. J. S.; Zeobisch, E. G.; Healy, E. A.; Stewart, J. J. P. *J. Am. Chem. Soc.* **1985**, *107*, 3902.
(7) (a) Warshel, A.; Karplus, M. *J. Am. Chem. Soc.* **1972**, *94*, 5612. (b) Allinger, N. L.; Sprague, J. T. *J. Am. Chem. Soc.* **1973**, *95*, 3893. (c) Warshel, A.; Levitt, M. *J. Mol. Biol.* **1976**, *103*, 227. (d) Singh, U. C.; Kollman, P. A. *J. Comput. Chem.* **1986**, *7*, 718.
(8) Dewar, M. J. S.; Storch, D. M. *J. Am. Chem. Soc.* **1985**, *107*, 3898.
(9) (a) Karplus, M.; Porter, R. N.; Saima, R. D. *J. Chem. Phys.* **1965**, *43*, 3259. (b) Bunker, D. L.; Jacobson, B.S. *J. Am. Chem. Soc.* **1972**, *94*, 1843. (c) Warshel, A.; Karplus, M. *Chem. Phys. Lett.* **1972**, *17*, 7. (d) Wang, I.; Karplus, M. *J. Am. Chem. Soc.* **1973**, *95*, 8160–8164. (e) Warshel, A.; Weiss, R. M. *J. Am. Chem. Soc.* **1980**, *102*, 6218.
(10) (a) Kirkwood, J. G. *J. Chem. Phys.* **1935**, *3*, 300. (b) Zwanzig, R. W. *J. Chem. Phys.* **1954**, *22*, 1420. (c) Torrey, G. M.; Valleau, J. P. *Chem. Phys. Lett.* **1974**, *28*, 578.
(11) Fleishman, S.; Tidor, B.; Brooks, C. B.; Karplus, M. to be published.
(12) Jorgensen, W. L.; Ravimohan, C. *J. Chem. Phys.* **1985**, *83*, 3050.
(13) (a) Postma, J. P.; Berendsen, H. J. C.; Haak, J. R. *Faraday Symp. Chem. Soc.* **1982**, *17* 55. (b) Straatsma, T. P.; Berendsen, H. J. C.; Postma, J. P. M. *J. Chem. Phys.* **1986**, *85*, 6720. (c) Berendsen, H. J. C.; Postma, J. P. M.; van Gunsteren, W. In *Molecular Dynamics and Protein Structure*; Hermans, J., Eds.; Polycrystal Book Service: IL, 1985.
(14) Singh, U. C.; Brown, F.; Bash, P. A.; Kollman, P. *J. Am. Chem. Soc.* **1987**, *109*, 1607.
(15) Mezei, M.; Beveridge, D. L. *Ann. N. Y. Acad. Sci.* **1986**, *482*, 1.
(16) Pettitt, B. M.; Karplus, M. *Molecular Graphics and Design*; Burgen, A. S. V., Roberts, G. C. K., Tue, M. S., Eds.; Elsevier; 1986.
(17) Brooks, B. R.; Bruccoleri, R. E.; Olafson, B. D.; States, D. J.; Swaminathan, S.; Karplus, M. *J. Comput. Chem.* **1983**, *4*, 187.
(18) Field, M. J.; Bash, P. A.; Karplus, M. manuscript in preparation.
(19) MOPAC: A general purpose MNDO and MINDO/3 program. Stewart, J. J. P. Quantum Chemistry Program Exchange 455, 1986, Vol. 6, No. 391.
(20) Brooks, C. L.; III. Brünger, A. T.; Karplus, M. *Biopolymers* **1985**, *24*, 843.
(21) Brünger, A.; Brooks, C. L., III, Karplus, M. *Proc. Natl. Acad. Sci. U.S.A.* **1985**, *82*, 8458.
(22) Jorgensen, W. L.; Chandrasekhar, J.; Madura, J.; Impey, R. W.; Klein, M. L. *J. Chem. Phys.* **1983**, *79*, 926.

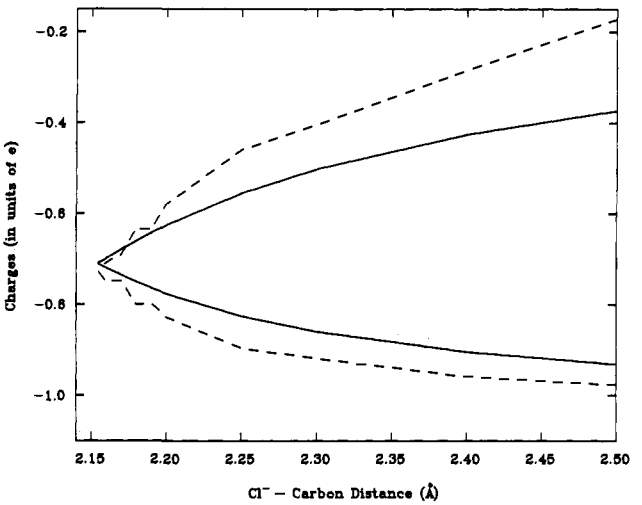

Figure 1. Comparison of average gas phase and solution charge transfer along the reaction coordinate for $Cl^- + CH_3Cl$. Values of Mulliken charges for the attacking Cl^- (lower curves) and the Cl (upper curves) of CH_3Cl are shown: (—) gas phase, (- - -) solution. The gas-phase analysis was done by minimizing each configuration with the Cl^- and C fixed at positions along the reaction pathway. The corresponding charge distributions were determined in solution by placing each of the minimized $Cl'\cdots CH_3Cl''$ complexes in a solvent water sphere with stochastic boundary molecular dynamics (see text) and doing dynamics runs at 300 K with 1 ps of equilibration followed by 2 ps of data collection; the Cl′ and C are fixed at their initial positions in all the simulations, and the Cl″ was also fixed for configurations near the transition state (i.e., for Cl′–C distances between 2.3 and 2.1545 Å).

the waters. Results of the calculations are given in Table I. For this reaction the free energy change and solvent effect in the reaction are insensitive to the inclusion of van der Waals parameters in the (qm),(mm) terms or the choice of quantum mechanical model. The results for the gas phase and solution are in satisfactory agreement with experimental estimates[23,25] and ab initio plus molecular mechanics calculations.[1]

To investigate the effect of solvation on the charge transfer during the reaction, we have compared the Mulliken populations obtained from gas-phase and solution simulations of the Cl^-,CH_3Cl system. The charges are shown in Figure 1. The charge transfer in solution lags behind that found in the gas phase due to the stabilization of the more asymmetric charge distribution by interaction with the solvent. This is in accord with the fact that the free energy of interaction between an ion and a dipolar solvent varies approximately quadratically with the charge on the ion.[26]

The present approach to potential surfaces of reactions in solution makes it possible to perform combined quantum, molecular mechanics calculations with molecular dynamics in large systems. The method avoids the need for extensive parameter fitting of the reaction pathway and permits one to obtain results concerning the effect of the solvent on the electronic structure of the solute. Applications to inhibitor binding and to enzymatic and solution reactions are in progress.

Acknowledgment. We thank J. J. P. Stewart for making the MOPAC program available to us. This work was supported in part by a grant from the National Science Foundation. Supercomputer resources were utilized at the San Diego Supercomputer Center. P. A. Bash is a Damon Runyon–Walter Winchell Cancer Fund Postdoctoral Fellow.

Registry No. MeCl, 74-87-3.

(23) Albery, W. J.; Kreevoy, M. M. *Adv. Phy. Org.* **1978**, *16*, 87.
(24) Dougherty, R. C.; Roberts, J. D. *Org. Mass. Spectrom.* **1974**, *8*, 77.
(25) Pellerite, M. J.; Brauman, J. I. *J. Am. Chem. Soc.* **1983**, *105*, 2672 and references therein.
(26) Yu, H.; Karplus, M. *J. Chem. Phys.*, submitted for publication.
(27) Arshadi, M.; Yamdagni, R.; Kebarle, P. *J. Phys. Chem.* **1970**, *74*, 1475.

Divalent Titanium Chemistry. Synthesis, Reactivity, and X-ray and Neutron Diffraction Studies of $Ti(BH_4)_2(dmpe)_2$ and $Ti(CH_3)_2(dmpe)_2$

James A. Jensen,[1a] Scott R. Wilson,[1a] Arthur J. Schultz,[1b] and Gregory S. Girolami*[1a]

School of Chemical Sciences
The University of Illinois at Urbana—Champaign
Urbana, Illinois 61801
Chemistry and Materials Science Divisions
Argonne National Laboratory
Argonne, Illinois 60439

Received June 26, 1987

Low valent organotitanium complexes have been implicated as Ziegler–Natta olefin polymerization catalysts[2] and as stoichiometric reagents in organic synthesis.[3] However, very few low-valent alkyls of titanium have been reported, and, in particular, the divalent oxidation state of titanium is virtually unexplored.[4,5] We now report the synthesis and characterization of the unusual divalent tetrahydroborate complex $Ti(BH_4)_2(dmpe)_2$, **1**, and its conversion to the methyl compound $Ti(CH_3)_2(dmpe)_2$, **2**. Complex **2** is unique among octahedral complexes of the 3d metals in being low-spin *within* the t_{2g} manifold and exhibits very unusual NMR features for the titanium methyl group.

The reaction of $TiCl_2(dmpe)_2$[5] with excess $LiBH_4$ in diethyl ether gives dark red crystals of the divalent tetrahydroborate complex $Ti(\eta^2\text{-}BH_4)_2(dmpe)_2$, **1**, after crystallization from toluene.[6]

$$TiCl_2(dmpe)_2 + 2LiBH_4 \rightarrow \underset{\mathbf{1}}{Ti(\eta^2\text{-}BH_4)_2(dmpe)_2} + 2LiCl$$

Complex **1** is paramagnetic with two unpaired electrons; this unfortunately prevents observation of the BH_4^- protons in the ^1H NMR spectrum. While the IR spectrum in the B–H stretching region is diagnostic of a bidentate bonding mode, the $\sim$110-cm^{-1} separation between the ν_{B-H}(terminal) and ν_{B-H}(bridging) modes is smaller than in all other transition-metal tetrahydroborate complexes[7] and is indicative of an unusually weak Ti–BH_4 interaction.[8] This suggestion is confirmed by the X-ray crystal structure of $Ti(BH_4)_2(dmpe)_2$ (Figure 1a)[9] which reveals that the Ti–H_b distances of 2.06 (2) Å are rather long and that the four

(1) (a) University of Illinois. (b) Argonne National Laboratory.
(2) (a) Boor, J. *Ziegler–Natta Catalysts and Polymerizations*; Academic Press: New York, 1979. (b) Gavens, P. D.; Bottrill, M.; Kelland, J. W.; McMeeking, J. *Comprehensive Organometallic Chemistry*; Wilkinson, G., Stone, F. G. A., Abel, E. W., Eds.; Pergamon Press: New York, 1982; Chapter 22–5. (c) Sinn, H.; Kaminsky, W. *Adv. Organomet. Chem.* **1980**, *18*, 99–149.
(3) (a) McMurray, J. E. *Acc. Chem. Res.* **1983**, *16*, 405–411. (b) Reetz, M. T. *Organotitanium Reagents in Organic Synthesis*; Springer-Verlag: New York, 1986.
(4) (a) Sikora, D. J.; Macomber, D. W.; Rausch, M. D. *Adv. Organomet. Chem.* **1986**, *25*, 317–379. (b) Girolami, G. S.; Wilkinson, G.; Thornton-Pett, M.; Hursthouse, M. B. *J. Chem. Soc., Dalton Trans.* **1984**, 2347–2350. (c) Kool, L. B.; Rausch, M. D.; Alt, H. G.; Herberhold, M.; Thewalt, U.; Wolf, B. *Angew. Chem., Int. Ed. Engl.* **1985**, *24*, 394–401. (d) Alt, H. G.; Engelhardt, H. E.; Rausch, M. D.; Kool, L. B. *J. Am. Chem. Soc.* **1985**, *107*, 3717–3718. (e) Palmer, G. T.; Basolo, F.; Kool, L. B.; Rausch, M. D. *J. Am. Chem. Soc.* **1986**, *108*, 4417–4427. (f) Blenkers, J.; Hessen, B.; van Bolhuis, F.; Wagner, A. J.; Teuben, J. H. *Organometallics* **1987**, *6*, 459–469.
(5) Girolami, G. S.; Wilkinson, G.; Galas, A. M. R.; Thornton-Pett, M.; Hursthouse, M. B. *J. Chem. Soc., Dalton Trans.* **1985**, 1339–1348.
(6) $Ti(BH_4)_2(dmpe)_2$: ^1H NMR (C_6D_6, 15 °C) δ 11.39 (PCH_2, fwhm = 770 Hz), -2.35 (PCH_3, fwhm = 290 Hz); IR (Nujol) 2332 s, 2297 s, 2220 s, 2138 m, 2062 w cm^{-1}.
(7) Marks, T. J.; Kolb, J. R. *Chem. Rev.* **1977**, *77*, 263–293.
(8) For titanium(III) tetrahydroborate complexes, see: (a) Jensen, J. A.; Girolami, G. S. *J. Chem. Soc., Chem. Commun.* **1986**, 1160–1162. (b) Melmed, K. M.; Coucouvanis, D.; Lippard, S. J. *Inorg. Chem.* **1973**, *12*, 232–236. (c) Franz, K.; Fusstetter, H.; Noth, H. *Z. Anorg. Allg. Chem.* **1976**, *427*, 97–113. (d) Semenenko, K. N.; Lobkovskii, E. B.; Shumakov, A. I. *J. Struct. Chem. USSR* **1976**, *17*, 912–914.
(9) Crystal data (T = 299 K): space group $P2_1/n$, with a = 9.404 (2) Å, b = 13.088 (2) Å, c = 9.466 (2) Å, β = 96.12 (1)°, V = 1158.4 (4) Å^3; Z = 2; R_F = 0.036, R_{wF} = 0.035 for 168 variables and 2139 unique data for which $I > 2.58\sigma(I)$. Hydrogen atom positions were refined with independent isotropic thermal coefficients.

0002-7863/87/1509-8094$01.50/0